

Transverse momentum spectra of D and B mesons in hadron collisions at high energies

G. I. LYKASOV¹, Z. M. KARPOVA¹, M. N. SERGEENKO² and V. A. BEDNYAKOV¹

¹ *Joint Institute for Nuclear Research - Dubna 141980, Moscow region, Russia*

² *State University of Transport - 34 Kirov Street, Gomel 246653, Belarus*

PACS 14.40.Lb – Charmed mesons

PACS 14.65.Dw – Charmed quarks

PACS 25.20.Lj – Inelastic scattering: many particle final states

Abstract. - Transverse momentum spectra of charmed and beauty mesons produced in proton-proton and proton-antiproton collisions at high energies are analyzed within the modified quark-gluon string model (QGSM) including the internal motion of quarks in colliding hadrons. It is shown that this approach can describe rather satisfactorily the experimental data at not large values of the transverse momentum where the NLO QCD calculation has a big uncertainty. We also show that using both the QGSM and the NLO QCD one can describe these data in a wide region of transverse momenta and give some predictions for the future LHC experiments.

Introduction. – Various approaches of perturbative QCD including the next-to-leading order calculations (NLO QCD) have been applied to construct distributions of quarks in a proton. The theoretical analysis of the lepton deep inelastic scattering (DIS) off protons and nuclei provides rather realistic information on the distribution of light quarks like u, d, s in a proton. However, to find a reliable distribution of heavy quarks like $c(\bar{c})$ and especially $b(\bar{b})$ in a proton describing the experimental data on the DIS is a non-trivial task. It is mainly due to small values of D and B meson yields in the DIS at existing energies. Even at the Tevatron energies the B -meson yield is not so large. At LHC energies the multiplicity of these mesons produced in pp collisions will be significantly larger. Therefore one can try to extract a new information on the distribution of these heavy quarks in a proton. In this paper we suggest to study the distribution of heavy quarks like $c(\bar{c})$ and $b(\bar{b})$ in a proton from the analysis of the future LHC experimental data.

The multiple hadron production in hadron-nucleon collisions at high energies and large transfers is usually analyzed within the hard parton scattering model (HPSM) suggested in [1, 2]. This model was applied to the charmed meson production both in proton-proton and meson-proton interactions at high energies, see for example [3]. The HPSM is significantly improved by applying the QCD parton approach implemented in the modified minimal-subtraction renormalization and factoriza-

tion scheme. The first calculation scheme is the so-called massive scheme or fixed-flavor-number scheme (FFNS) developed in [4]- [7]. In this approach the number of active flavors in the initial state is limited to $n_f = 4$, e.g., $u(\bar{u}), d(\bar{d}), s(\bar{s})$ and $c(\bar{c})$ quarks being the initial partons, whereas the $b(\bar{b})$ quark appears only in the final state. In this case the beauty quark is always treated as a heavy particle, not as a parton. In this scheme the mass of heavy quarks acts as a cutoff parameter for the initial-state and final-state collinear singularities and sets the scale for perturbative calculations. Actually, the FFNS with $n_f = 4$ is limited to a rather small range of transverse momenta p_t of produced D or B mesons less than the masses of c or b quarks. In this scheme the terms $m_{c,b}^2/p_t^2$ are fully included.

Another approach is the so-called zero-mass variable-flavor-number scheme (ZM-VFNS), see [8]- [10] and references therein. It is the conventional parton model approach, the zero-mass parton approximation is also applied to the b quark, although its mass is certainly much larger than the asymptotic scale parameter Λ_{QCD} . In this approach the $b(\bar{b})$ quark is treated as an incoming parton originating from colliding hadrons. This approach can be used in the region of large transverse momenta of produced charmed or beauty mesons, e.g., at $p_t \geq m_{c,b}$. Within this scheme the terms of order $m_{c,b}^2/p_t^2$ can be neglected. Recently the experimental inclusive p_t spectra of B mesons in $p\bar{p}$ collisions obtained by the CDFII Collaboration [12, 13]

at the Tevatron energy $\sqrt{s} = 1.96$ TeV in the rapidity region $-1 \leq y \leq 1$ have been described rather satisfactorily within this ZM-VFNS approach in [11] at $p_t \geq 10$ GeV/c using the non-perturbative structure functions. In another kinematic region, e.g., at 2.5 GeV/c $\leq p_t \leq 10$ GeV/c, the FFNS model allowed the CDFII data to be described without using fragmentation functions of b quarks to B mesons. Both these schemes have some uncertainties related to the renormalization parameters.

In this paper we study the charmed and beauty meson production within the QGSM [14] or the dual parton model (DPM) [15]. based on the $1/N$ expansion in QCD [16, 17]. We show that this approach can be applied rather successfully at not very large values of p_t .

General formalism. – Let us analyze the D -meson production in the pp and $p\bar{p}$ collisions within the QGSM including the transverse motion of quarks and diquarks in colliding protons [19]. As is known, the cylinder type graphs for the pp collision presented in fig. 1 make the main contribution to this process [14]. The left diagram of fig. 1, the so-called one-cylinder graph, corresponds to the case where two colorless strings are formed between the quark/diquark ($q/q\bar{q}$) and the diquark/quark (qq/q) in colliding protons; then, after their breakup, $q\bar{q}$ pairs are created and fragmented to a hadron, for example, D meson. The right diagram of fig. 1, the so-called multicylinder graph, corresponds to creation of the same two colorless strings and many strings between sea quarks/antiquarks q/\bar{q} and sea antiquarks/quarks \bar{q}/q in the colliding protons.

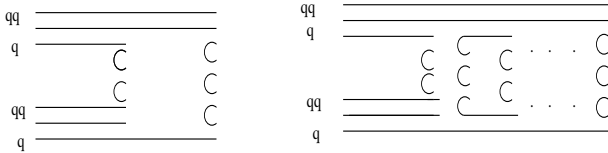


Fig. 1: The one-cylinder graph (left diagram) and the multicylinder graph (right diagram) for the inclusive $pp \rightarrow hX$ process.

The general form for the invariant inclusive hadron spectrum within the QGSM is [18, 19]

$$E \frac{d\sigma}{d^3\mathbf{p}} \equiv \frac{2E^*}{\pi\sqrt{s}} \frac{d\sigma}{dx dp_t^2} = \sum_{n=1}^{\infty} \sigma_n(s) \phi_n(x, p_t), \quad (1)$$

where E, \mathbf{p} are the energy and the three-momentum of the produced hadron h in the laboratory system (l.s.) of colliding protons, E^*, s are the energy of h and the square of the initial energy in the c.m.s of pp , x, p_t are the Feynman variable and the transverse momentum of h ; σ_n is the cross section for production of the n -Pomeron chain (or $2n$ quark-antiquark strings) decaying into hadrons, calculated within the “eikonal approximation” [20], the function $\phi_n(x, p_t)$ has the following form [19]:

$$\phi_n(x, p_t) = \int_{x^+}^1 dx_1 \int_{x^-}^1 dx_2 \psi_n(x, p_t; x_1, x_2), \quad (2)$$

where

$$\begin{aligned} \psi_n(x, p_t; x_1, x_2) = & (3) \\ & F_{qq}^{(n)}(x_+, p_t; x_1) F_{q\bar{v}}^{(n)}(x_-, p_t; x_2) / F_{q\bar{v}}^{(n)}(0, p_t) \\ & + F_{q\bar{v}}^{(n)}(x_+, p_t; x_1) F_{qq}^{(n)}(x_-, p_t; x_2) / F_{qq}^{(n)}(0, p_t) \\ & + 2(n-1) F_{q_s}^{(n)}(x_+, p_t; x_1) F_{\bar{q}_s}^{(n)}(x_-, p_t; x_2) / F_{q_s}^{(n)}(0, p_t). \end{aligned}$$

$$\text{and } x_{\pm} = 0.5(\sqrt{x^2 + x_t^2} \pm x), x_t = 2\sqrt{(m_h^2 + p_t^2)/s},$$

$$F_{\tau}^{(n)}(x_{\pm}, p_t; x_{1,2}) = \int d^2 k_t \tilde{f}_{\tau}^{(n)}(x_{1,2}, k_t) \tilde{G}_{\tau \rightarrow h} \left(\frac{x_{\pm}}{x_{1,2}}, k_t; p_t \right), \quad (4)$$

$$F_{\tau}^{(n)}(0, p_t) = \int_0^1 dx' d^2 k_t \tilde{f}_{\tau}^{(n)}(x', k_t) \tilde{G}_{\tau \rightarrow h}(0, p_t) = \tilde{G}_{\tau \rightarrow h}(0, p_t).$$

Here τ means the flavor of the valence (or sea) quark or diquark, $\tilde{f}_{\tau}^{(n)}(x', k_t)$ is the quark distribution function depending on the longitudinal momentum fraction x' and the transverse momentum k_t in the n -Pomeron chain; $\tilde{G}_{\tau \rightarrow h}(z, k_t; p_t) = z \tilde{D}_{\tau \rightarrow h}(z, k_t; p_t)$, $\tilde{D}_{\tau \rightarrow h}(z, k_t; p_t)$ is the fragmentation function (FF) of a quark (antiquark) or diquark of flavor τ into a hadron h (D meson in our case). We present the quark distributions and the FF in the factorized forms $\tilde{f}_{\tau}(x, k_t) = f_{\tau}(x)g_{\tau}(k_t)$, and, according to [22], $\tilde{G}_{\tau \rightarrow h}(z, k_t; p_t) = G_{\tau \rightarrow h}(z)\tilde{g}_{\tau \rightarrow h}(\tilde{k}_t)$, where $\tilde{\mathbf{k}}_t = \mathbf{p}_t - z\mathbf{k}_t$. We take the quark distributions $f_{\tau}(x)$ and the FF $G_{\tau \rightarrow h}(z)$ obtained within the QGSM from [18, 23, 24], whereas their k_t distributions are chosen in the form suggested in [21, 22]

$$g_{\tau}(k_t) = (B_q^2/2\pi) \exp(-B_q(\sqrt{k_t^2 + m_D^2} - m_D)), \quad (6)$$

$$\tilde{g}_{\tau \rightarrow h}(\tilde{k}_t) = (B_c^2/2\pi) \exp(-B_c(\sqrt{\tilde{k}_t^2 + m_D^2} - m_D)). \quad (7)$$

After the integration of eq. (5) over $d^2 k_t$ we have, according to [22],

$$F_{\tau}^{(n)}(x_{\pm}, p_t; x_{1,2}) = \tilde{f}_{\tau}^{(n)}(x_{1,2}) G_{\tau \rightarrow h}(z) I_n(z, p_t), \quad (8)$$

where $z = x_{\pm}/x_{1,2}$, $I_n(z, p_t) = B_z^2/(2\pi(1 + B_z m_D)) \exp(-B_z(m_D t - m_D))$, $m_{Dt}^2 = p_t^2 + m_D^2$; $B_z = B_c/(1 + n\rho z^2)$, $\rho = B_c/B_q$. The function B_z also can be presented in the equivalent form $B_z = B_q/(\tilde{\rho} + n z^2)$,

where $\tilde{\rho} = B_q/B_c$. The differential cross section $d\sigma/dp_t^2$ for D mesons produced in pp collisions is written in the form [18]

$$\frac{d\sigma}{dp_t^2} = \frac{\pi}{2} \sqrt{s} \sum_{n=1}^{\infty} \sigma_n(s) \int \phi_n(x, p_t) \frac{dx}{E^*}. \quad (9)$$

The production of heavy mesons like D - and B -mesons in proton-antiproton collisions at high energies is usually analyzed within the different schemes of QCD. To study these processes within the QGSM we have to include at least one additional graph corresponding to the creation of three chains between quarks in the initial proton and antiquarks in the colliding antiproton, as is illustrated in fig. 2 (bottom diagram).

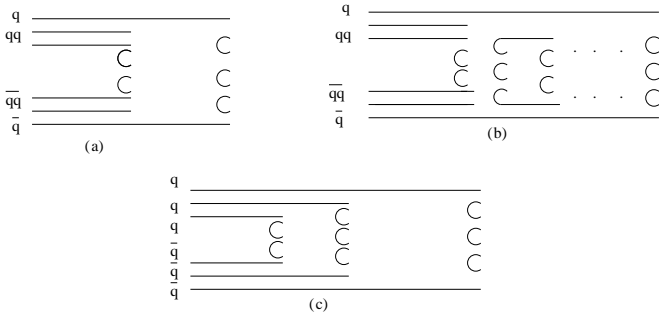


Fig. 2: The one-cylinder graph (left diagram) and the multi-cylinder graph (right diagram), and the three-chains graph (down diagram) for the $p\bar{p} \rightarrow hX$ inclusive process.

The left and right diagrams in fig. 2 are similar to the one-cylinder and multicylinder diagrams for the pp collision in fig. 1 with a following difference. In the $p\bar{p}$ collision two colorless strings between quark/diquark ($q/q\bar{q}$) in the initial proton and antiquark/antidiquark ($\bar{q}/\bar{q}\bar{q}$) are created. Many quark-antiquark ($q - \bar{q}$) strings for $p\bar{p}$ collision (fig. 2, right diagram) are the same as for the pp collision (fig. 1, right diagram). Therefore, the invariant inclusive spectrum of hadrons produced in the $p\bar{p}$ collision calculated within the QGSM has the following form:

$$E \frac{d\sigma^{p\bar{p}}}{d^3\mathbf{p}} = \sigma_1(s) \left((1 - \omega) \phi_1^{p\bar{p}}(x, p_t) + \omega \tilde{\phi}(x, p_t) \right) + \sum_{n=2}^{\infty} \sigma_n(s) \phi_n^{p\bar{p}}(x, p_t) \quad (10)$$

where $1 - \omega$ is the probability of contribution of the cut one-cylinder (one-Pomeron exchange) and cut multi-cylinder (multi-Pomeron exchanges) graphs (the left and right diagrams in fig. 2), whereas ω is the probability of the contribution of the three-chain diagram to the inclusive spectrum. The value of ω can be estimated as the ratio of the $p\bar{p}$ annihilation cross section $\sigma_{p\bar{p}}^{ann}$ to the total $p\bar{p}$ cross section $\sigma_{p\bar{p}}^{tot}$. The cross section $\sigma_{p\bar{p}}^{tot}$ is well known in the wide range of the initial energies to the

Tevatron energy, whereas experimental data on $\sigma_{p\bar{p}}^{ann}$ are available only for the antiproton initial energy about 10 GeV, see [26] and references therein. However, some theoretical predictions, for example [27, 28], show that asymptotically $\sigma_{p\bar{p}}^{ann}$ goes to about 2 – 4 mb. It corresponds to $\omega \simeq \sigma_{p\bar{p}}^{ann}/\sigma_{p\bar{p}}^{tot} < 0.1$ at the Tevatron energy. Note that in addition to the graph of fig 2c there can be diagrams consisting of these three chains and multicylinder chains between sea quarks and antiquarks. However, as our estimations show, their contribution to the inclusive spectrum is much smaller than the contribution from the three-chain graph (fig 2c). Therefore we neglect it. The form for the function $\phi_n^{p\bar{p}}(x, p_t)$ is similar to $\phi_n(x, p_t)$ entering into (3) by replacing $F_{q_v}^{(n)}(x_-, p_t; x_2)$, $F_{q_v}^{(n)}(0, p_t)$ to $F_{q\bar{q}}^{(n)}(x_-, p_t; x_2)$, $F_{q\bar{q}}^{(n)}(0, p_t)$ respectively, and replacing $F_{q\bar{q}}^{(n)}(x_-, p_t; x_2)$, $F_{q\bar{q}}^{(n)}(0, p_t)$ to $F_{\bar{q}}^{(n)}(x_-, p_t; x_2)$ and $F_{\bar{q}}^{(n)}(0, p_t)$ respectively. The additional term $\tilde{\phi}(x, p_t)$ in (11) has the following form

$$\tilde{\phi}(x, p_t) = 3\tilde{F}_{q_v}(x_+, p_t)\tilde{F}_{\bar{q}_v}(x_-, p_t)/\tilde{F}_q(0, p_t), \quad (11)$$

where $\tilde{F}_{q_v(\bar{q}_v)}(x_{\pm}, p_t) = F_{q_v(\bar{q}_v)}^{(n=1)}(x_{\pm}, p_t)$ and $\tilde{F}_q(0, p_t) = F_q^{(n=1)}(0, p - t)$.

Results and discussion. – To illustrate our approach we present in figs. 3,4 the inclusive spectrum $d\sigma/dp_t^2$ of D^0 -mesons produced in the reaction $pp \rightarrow D^0X$ at $\sqrt{s} = 27.4$ GeV as a function of p_t^2 given by eq.(9). One can see from fig. 3 that the use of different values for the intercept $\alpha_{\Psi}(0)$ leads mainly to the shift of the theoretical lines along the y axis. figs. 3,4 show a satisfactory description of the experimental data obtained by the NA27 Collaboration [25] at both values for the linear Ψ -trajectory when $\alpha_{\Psi}(0) = -2.18$ and for the nonlinear one when $\alpha_{\Psi}(0) = 0$. Unfortunately, the experimental data are very poor because of big error bars; therefore, we cannot get new information on the Ψ -trajectory.

The inclusive p_t spectra of D^0 and B^+ mesons produced in the $p\bar{p}$ collision at the Tevatron energy $\sqrt{s} = 1.96$ TeV are presented in figs. 5,6. The hatched regions in figs. 5,6 show the calculations within the NLO QCD including uncertainties [30]. The dashed lines ($\omega = 0$) and dash-dotted curves ($\omega = 0.1$) in figs. 5,6 correspond to our best fit obtained within the QGSM-I calculations using the parameter values $B_c = 0.65(\text{GeV}/c)^{-1}$ for D mesons (fig. 5) and $B_c = 0.55(\text{GeV}/c)^{-1}$ for B mesons (fig. 6), and $\rho \equiv B_c/B_q = 3.1$ [22], e.g., $B_q \simeq 0.2(\text{GeV}/c)^{-1}$. However, the value used for the slope B_q of the quark distribution as a function of k_t is too small. Therefore, we also calculated these p_t -spectra taking the more realistic values $B_q = 4.5(\text{GeV}/c)^{-1}$ at the Tevatron energy and $B_q = 4(\text{GeV}/c)^{-1}$ at the LHC energy that correspond approximately to $\langle k_t \rangle \simeq 0.45$ GeV/c and $\langle k_t \rangle \simeq 0.5$ GeV/c respectively. This calculation (QGSM-II) is shown by the solid lines in figs. 5,6 and in figs. 7,8. Accord-

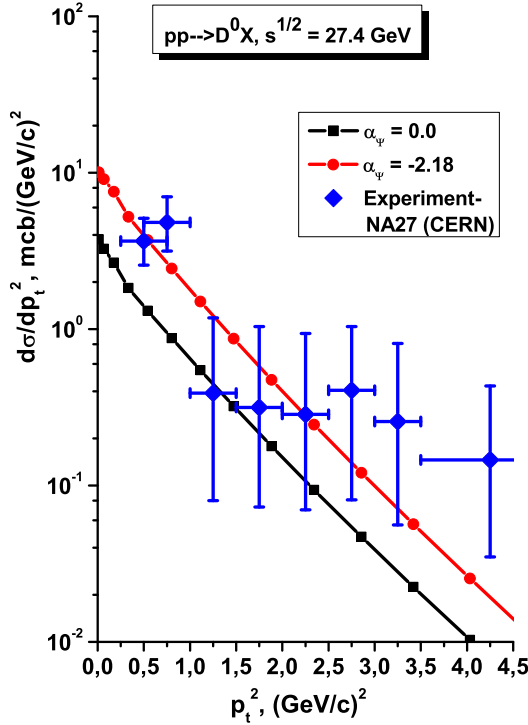


Fig. 3: The inclusive spectrum for D^0 mesons produced in the pp collision at $\sqrt{s} = 27.4$ GeV as a function of p_t^2 , see details in [22].

ing to the experimental data, the mean transverse momentum of hadrons produced in hadron collisions slowly increases as the energy increases. Therefore, the internal transverse momentum of the quark in the proton can also slowly increase. In fact, we have only one free parameter $\tilde{\rho} \equiv 1/\rho = B_q/B_c$ which is experimentally unknown, whereas B_q is directly related to the mean transverse momentum of the quark in the proton or antiproton which is more or less known experimentally. To describe the experimental data on the p_t -spectra in the p_t region where the NLO QCD calculation has a big uncertainty we chose $\tilde{\rho} = 7$ both for the Tevatron and the LHC energies. When $B_c < 1$ (GeV/c) $^{-1}$, eq.(7) can be approximately presented in the form $\tilde{g}_{\tau \rightarrow h}(k_t) \simeq a^2/(a^2 + k_t^2)$ at $k_t^2 < 2m_D$, where $a = \sqrt{2m_D/B_c}$. This form is similar to the form for the FF of heavy quarks obtained within the perturbative QCD, see for example [29]. Note that the function $I_n(z, p_t)$ in eq.(8) was obtained in [19, 22] on the assumption of the consequent sharing of the transverse momentum p_t in the proton (antiproton) between n -Pomeron chains. It allowed us to describe rather satisfactorily the experimental data on the inclusive p_t spectra of charmed and beauty mesons produced in $p\bar{p}$ collisions at moderate values of the transverse momentum $p_t < 10$ GeV/c. It is illustrated in figs. 5,6. We also use $\lambda = 2\alpha'_{D^*(B^*)}(0) < p_t^2 >$, $\alpha'_{D^*(B^*)}(0) \simeq 0.5$ (GeV/c) $^{-2}$ is the slope of the D^* or B^*

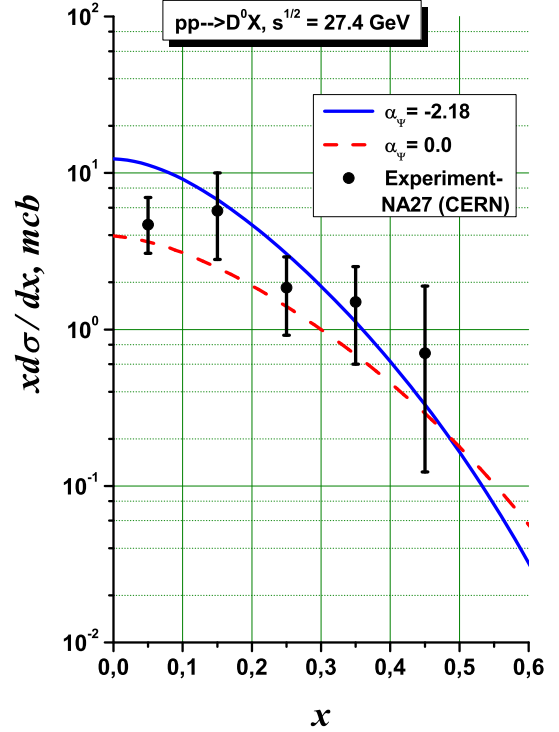


Fig. 4: The inclusive spectrum for D^0 mesons produced in the pp collision at $\sqrt{s} = 27.4$ GeV as a function of x , see details in [22].

Regge trajectory, $< p_t^2 > \simeq 5$ (GeV/c) 2 is the mean transverse momentum squared of the D meson or B meson that was found from the CDFII experimental data. Note that our calculation showed that the contribution of the three-chain graph (fig. 2c) is very small at the Tevatron energy. It is due to small values of the $p\bar{p}$ annihilation cross section at very high energies [27, 28].

The predictions for inclusive p_t spectra of D^0 and B^+ mesons produced in the pp collision at LHC energies and the NLO QCD calculation for the produced charmed quarks [31] are presented in figs. 7,8.

The solid lines correspond to our calculations within the QGSM-II, whereas the hatched regions show the calculations within the NLO QCD including uncertainties [31]. A big difference between the QGSM and NLO QCD calculations at $p_t > 10$ GeV/c for D and B mesons can be due to the following. First, the NLO QCD calculation [31] does not include the hadronization of quarks to heavy mesons, whereas the QGSM calculation includes it. Second, we do not include the contribution of gluons and their hard scatterings off quarks and gluons which can be sizable at large values of p_t .

Conclusion. – We have shown that the modified QGSM including the intrinsic longitudinal and transverse motion of quarks (antiquarks) and diquarks in colliding

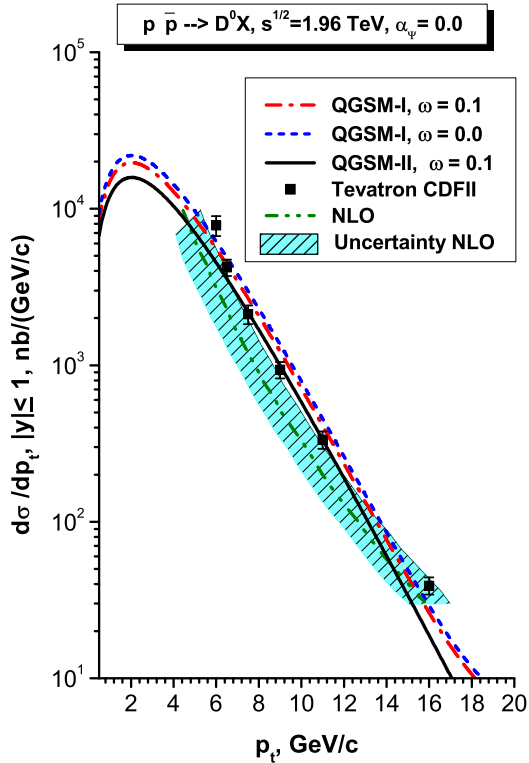


Fig. 5: The inclusive p_t -spectrum for D^0 mesons produced in the $p\bar{p}$ collision at the Tevatron energy $\sqrt{s} = 1.96$ TeV obtained within the QGSM (the solid and dashed lines) and within the NLO QCD [30] (the hatched regions); QGSM-I: $B_q \simeq 0.18(\text{GeV}/c)^{-1}$, $\tilde{\rho} \simeq 0.32$; QGSM-II: $B_q = 4.5(\text{GeV}/c)^{-1}$, $\tilde{\rho} = 7$.

protons allowed us to describe rather satisfactorily the existing experimental data on inclusive spectra of D mesons produced in pp collisions and to make some predictions for similar spectra at LHC energies. To verify whether these predictions can be reliable or not we apply the QGSM to the analysis of charmed and beauty meson production in proton-antiproton collisions at Tevatron energies including graphs like those in fig. 2c corresponding to annihilation of quarks and antiquarks in colliding p and \bar{p} , and production of D -mesons.

We got a satisfactory QGSM-II description ($p_t < 10$ GeV/c) of the experimental data on p_t spectra of D^0 and B^+ mesons produced in the $p\bar{p}$ collisions which were obtained by the CDFII Collaboration at the Tevatron [30]. At larger values of p_t the calculations within the NLO of QCD [4, 8] result in a better description of these data. It can be due to the contribution of gluons inside the colliding proton and antiproton which can interact with other gluons and quarks (antiquarks) and fragmentate to charmed mesons. This effect is not taken into account in the presented QGSM. Therefore, the QGSM including the internal transverse momenta of partons in the proton (let

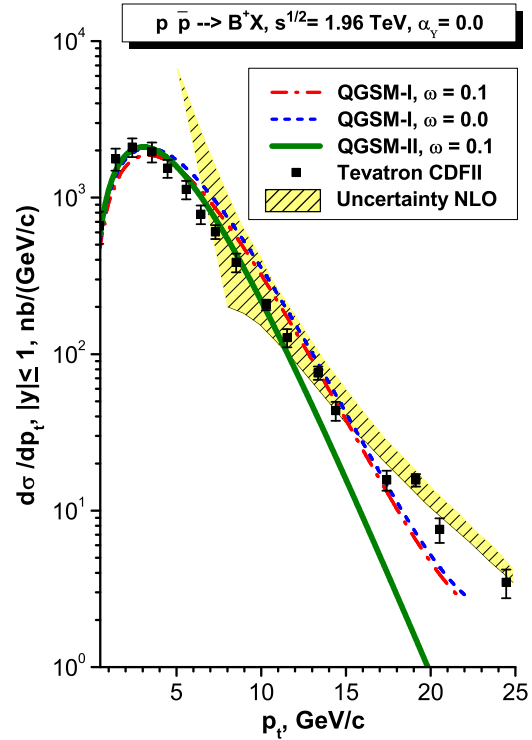


Fig. 6: The inclusive p_t -spectrum for B^+ mesons produced in the $p\bar{p}$ collision at the Tevatron energy $\sqrt{s} = 1.96$ TeV obtained within the QGSM (the solid and dashed lines) and within the NLO QCD [30] (the hatched regions); QGSM-I: $B_q \simeq 0.21(\text{GeV}/c)^{-1}$, $\tilde{\rho} \simeq 0.32$; QGSM-II is the same as in Fig (5).

us call it the “soft QCD”) allows us to describe the inclusive p_t spectra of heavy mesons produced in pp and $p\bar{p}$ collisions at high energies at not very large values of p_t . To describe these spectra and make some predictions for the future LHC experiments in a wide region of transverse momenta one can combine the “soft QCD” at small values of p_t with the NLO QCD at large p_t .

We found that the p_t spectra of D and B mesons calculated within the QGSM are almost insensitive to the form of the sea $c(\bar{c})$ and $b(\bar{b})$ quark distributions in colliding protons/antiprotons. To find a new information on it we intend to study the charm and beauty hadron production in pp collisions at small scattering angles.

We thank W. Cassing, M. Deile, A. V. Efremov, K. Eggert, D. Elia, S.B.Gerasimov, A. B. Kaidalov, B. Z. Kopeliovich, A. D. Martin, M. Poghosyan, K. Safarik, J. Schukraft, V. V. Uzhinsky and D. Weber for very useful discussions. This work was supported in part by the High Energy Foundation and the World Science Agency and the RFBR grant N 08-02-01003.

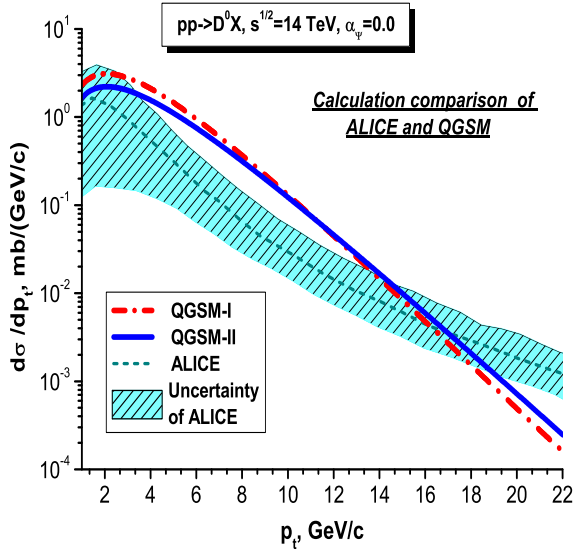


Fig. 7: The inclusive spectrum for D^0 mesons produced in the pp collision at the LHC energy $\sqrt{s} = 14$ TeV obtained within the QGSM for charmed mesons and the NLO QCD for c quarks [31]; QGSM-I corresponds to the same QGSM-I as in Fig 5; QGSM-II: $B_q = 4$. $(\text{GeV}/c)^{-1}$, $\tilde{\rho} = 7$.

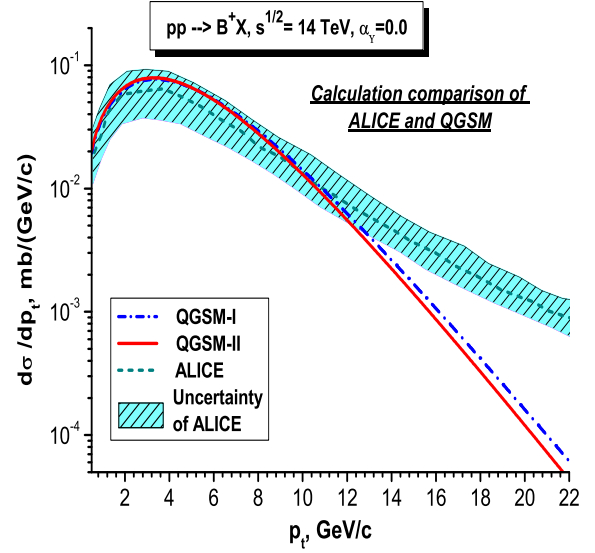


Fig. 8: The inclusive spectrum for B^+ mesons produced in the pp collision at the LHC energy $\sqrt{s} = 14$ TeV obtained within the QGSM for beauty mesons and the NLO QCD for single b quarks [31]; QGSM-I corresponds to the same QGSM-I as in Fig (6); QGSM-II is the same as in Fig 7.

REFERENCES

- [1] EFREMOV A. V., *Yad. Fiz.*, **19** (1974) 179.
- [2] FIELD R. D. and FEYMAN R. P., *Phys. Rev. D*, **15** (1977) 2590; FIELD R. D., FEYMAN R. P. and FOX G. C., *Nucl. Phys. B*, **128** (1977) 1.
- [3] BEDNYAKOV V.A., *Mod.Phys.Lett. A*, **10** (1995) 61.
- [4] NASSON P., DAWSON S. and ELLIS R. K., *Nucl. Phys. B*, **303** (1988) 607; **327** (1989) 49; **335** (1989) 260E.
- [5] BEENAKKER W., KUIJF H., VAN NEERVEN W. L. and J. SMITH, *Phys.Rev. D*, **40** (1989)54.
- [6] BEENAKKER W., VAN NEERVEN W. L., MENG R., SCHULER G.A. and SMITH J., *Nucl. Phys. B*, **351** (1991) 507.
- [7] BOJAK I. and STRATMANN M., *Phys.Rev. D*, **67** (2003) 034010.
- [8] BINNEWIES J., KNIEHL B. A. and KRAMER G., *Phys.Rev. D*, **58** (1998) 034016.
- [9] KNIEHL B.A. & KRAMER G., *Phys.Rev. D*, **60** (1999) 014006.
- [10] CACCIARI M. and GRECO M., *Nucl. Phys. B*, **421** (1994) 530.
- [11] KNIEHL B. A., KRAMER G., SCHIENBEIN I. and SPIESBERGER H., hep-ph/075054392 preprint, 2007.
- [12] ACOSTA D., *et al.* (CDF COLLABORATION), *Phys. Rev. D*, **71** (2005) 032001.
- [13] ABULENCIA A., *et al.* (CDF COLLABORATION), *Phys.Rev. D*, **75** (2007) 012010.
- [14] KAIDALOV A. B., *Phys. Lett. B*, **116** (1982) 459; KAIDALOV A. B. and TER-MARTIROSYAN K. A., *Phys. Lett. B*, **117** (1982) 247.
- [15] CAPELLA A., SUKHATME U., TAN C. I., TRAN THAN VAN J., *Phys. Rep.*, **236** (1994) 225.
- [16] T'HOOFT G., *Nucl.Phys. B*, **72** (1974) 461.
- [17] VENEZIANO G., *Phys. Lett. B*, **52** (1974) 220.
- [18] KAIDALOV A. B. and PISKUNOVA O. I., *Z. Phys. C*, **30** (1986) 145.
- [19] LYKASOV G. I., ARAKELIAN G. H. and SERGEENKO M. N., *Phys. Part. Nucl.*, **30** (1999) 343; G. I. LYKASOV and SERGEENKO M. N., *Z. Phys. C*, **70** (1996) 455.
- [20] TER-MARTIROSYAN K. A., *Phys. Lett. B*, **44** (1973) 377.
- [21] VESELOV A. I., PISKUNOVA O. I., TER-MARTIROSYAN K. A., Moscow, ITEP-176 preprint, 1990.
- [22] LYKASOV G. I. and SERGEENKO M. N., *Z. Phys. C*, **56** (1992) 697.
- [23] SHABELSKY YU. M., *Yad. Fiz.*, **56** (1992) 2512.
- [24] PISKUNOVA O. I., *Yad. Fiz.*, **56** (1993) 176; **64** (2001) 392.
- [25] ANGULAR-BENITZER M., *et al.* (NA27 COLLABORATION), *Phys. Lett. B*, **189** (1987) 476; **201** (1988) 176.
- [26] V. V. UZHINSKY and A. S. GALOYAN, *hep-ph*, **0212369** (2002) 1.
- [27] GOSTMAN E. and NUSSINOV S., *Phys. Rev. D*, **22** (1980) 624.
- [28] KOPELIOVICH B. Z. and ZAKHAROV B. G. , *Phys. Lett.B*, **211** (1986) 221.
- [29] CACCIARI M. and GRECO M., *Phys. Rev. Lett.*, **73** (1994) 1586.
- [30] ACOSTA D., *et al.* (CDF COLLABORATION), *Phys. Rev. Lett.*, **91** (2003) 241804.
- [31] ALESSANDRO B., *et al.* (ALICE COLLABORATION), *J. Phys. G: Nucl. Part. Phys.*, **32** (2006) 1295.